AMERICAN SOCIETY FOR MICROBIOLOGY | Infection and Immunity®

MOLECULAR PATHOGENESIS

The Ethanolamine-Sensing Transcription Factor EutR Promotes Virulence and Transmission during *Citrobacter rodentium* Intestinal Infection

Carol A. Rowley,[a] Amber B. Sauder,[a] Melissa M. Kendall[a]

[a]Department of Microbiology, Immunology, and Cancer Biology, University of Virginia School of Medicine, Charlottesville, Virginia, USA

ABSTRACT Enteric pathogens exploit chemical and nutrient signaling to gauge their location within a host and control expression of traits important for infection. Ethanolamine-containing molecules are essential in host physiology and play important roles in intestinal processes. The transcription factor EutR is conserved in the *Enterobacteriaceae* and is required for ethanolamine sensing and metabolism. In enterohemorrhagic *Escherichia coli* (EHEC) O157:H7, EutR responds to ethanolamine to activate expression of traits required for host colonization and disease; however, the importance of EutR to EHEC intestinal infection has not been examined. Because EHEC does not naturally colonize or cause disease in mice, we employed the natural murine pathogen *Citrobacter rodentium* as a model of EHEC virulence to investigate the importance of EutR *in vivo*. EHEC and *C. rodentium* possess the locus of enterocyte effacement (LEE), which is the canonical virulence trait of attaching and effacing pathogens. Our findings demonstrate that ethanolamine sensing and EutR-dependent regulation of the LEE are conserved in *C. rodentium*. Moreover, during infection, EutR is required for maximal LEE expression, colonization, and transmission efficiency. These findings reveal that EutR not only is important for persistence during the primary host infection cycle but also is required for maintenance in a host population.

KEYWORDS *Citrobacter*, EHEC, enteric, ethanolamine, virulence

Nutrient and chemical signaling are fundamental for all cellular processes, including interactions between the mammalian host and the microbiota, which have a significant impact on health and disease. Bacteria respond to metabolites within a host to enhance growth and regulate expression of traits important for colonization (1). Ethanolamine (EA) is a component of phosphatidylethanolamine, an abundant and essential phospholipid in the cell membrane. The turnover of enterocytes and bacteria contributes to a continuously replenished source of EA in the gastrointestinal (GI) tract (2–4), suggesting that EA sensing is a reliable means of gauging the host intestinal environment. Indeed, *in vitro* and *in vivo* studies have revealed that EA influences growth and/or gene expression of diverse commensal and pathogenic bacteria (5–14).

The role of EA in activating virulence gene expression was first described for enterohemorrhagic *Escherichia coli* O157:H7 (EHEC) (15–17). EHEC is a foodborne pathogen that colonizes the colon and causes major outbreaks of bloody diarrhea and hemolytic-uremic syndrome (18). After ingestion, EHEC travels through the GI tract; upon reaching the colon, EHEC expresses virulence factors, including Shiga toxin and the locus of enterocyte effacement (LEE) pathogenicity island. Stx is a potent inhibitor of protein synthesis (19) that is responsible for the severe morbidity and mortality associated with EHEC (19). The LEE encodes a type III secretion system (T3SS) and most effectors required for formation of attaching and effacing lesions on enterocytes

Citation Rowley CA, Sauder AB, Kendall MM. 2020. The ethanolamine-sensing transcription factor EutR promotes virulence and transmission during *Citrobacter rodentium* intestinal infection. Infect Immun 88:e00137-20. https://doi.org/10.1128/IAI.00137-20.

Editor Manuela Raffatellu, University of California San Diego School of Medicine

Address correspondence to Melissa M. Kendall, melissakendall@virginia.edu.

Received 9 March 2020
Returned for modification 12 May 2020
Accepted 26 June 2020
Accepted manuscript posted online 6 July 2020
Published 19 August 2020

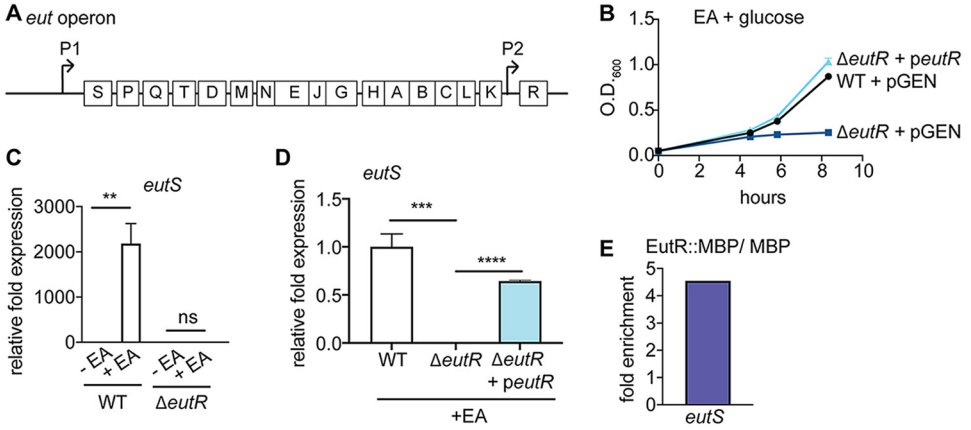

FIG 1 *C. rodentium* possesses a functional *eut* operon. (A) Schematic of the *eut* locus. (B) Growth curve of WT, Δ*eutR*, and complemented *C. rodentium* strains grown in minimal medium with EA ($n = 3$). (C) RT-qPCR of *eutS* expression in WT and Δ*eutR C. rodentium* strains grown in the absence or presence of EA ($n = 3$). (D) RT-qPCR of *eutS* expression in WT, Δ*eutR*, and complemented *C. rodentium* strains grown in the presence of EA ($n = 3$). (E) qPCR showing enrichment of *eutS* from *in vivo* ChIP of EutR::MBP compared to MBP ($n = 2$). Error bars represent standard deviations (SD). **, $P < 0.01$; ***, $P < 0.001$; ****, $P < 0.0001$. ns, not significant.

(20–27). AE lesions are characterized by effacement of microvilli and intimate attachment of EHEC to epithelial cells (28).

EHEC senses EA through the transcription factor EutR. EutR directly activates expression of the LEE and promotes expression of other regulatory factors and adhesins that contribute to virulence expression and adherence to epithelial cells (15–17). To date, the importance of EutR to EHEC virulence during infection of the mammalian GI tract has not been tested. This is mainly due to the lack of convenient animal models that recapitulate EHEC infection. In this study, we employed *Citrobacter rodentium* to examine the role of EutR in LEE expression and colonization during intestinal infection. *C. rodentium* is a natural murine pathogen that colonizes the cecum and distal colon in mice (29) and is commonly used as a murine model of EHEC infection (29–31). *C. rodentium* carries the LEE and forms AE lesions on epithelial cells (32). We demonstrate that EutR-dependent EA sensing and concomitant regulation of the LEE are conserved in EHEC and *C. rodentium*. Notably, EutR is required for robust *C. rodentium* colonization of the colon and transmission efficiency. These data underscore the importance of optimal control of virulence expression in pathogen transmission and persistence in a host population.

RESULTS AND DISCUSSION

***C. rodentium* possesses a functional *eut* operon.** In the *Enterobacteriaceae*, the *eut* locus is comprised of 17 genes (Fig. 1A) that code for transport and catabolism of EA, as well as a microcompartment that contains toxic breakdown products of EA metabolism (33–38). Despite the availability of EA in the intestine, at least a subset of enteric *E. coli* strains have acquired a large phage insertion between the genes encoding the EA ammonia lyase EutBC, resulting in the inability to metabolize EA (17, 39). Our data demonstrate that *C. rodentium* grows using EA as a nitrogen source (Fig. 1B), indicating that *C. rodentium* possesses a functional *eut* locus.

The last gene in the *eut* locus encodes the transcriptional regulator EutR, which is 96% similar at the amino acid level between EHEC and *C. rodentium* (see Fig. S1 in the supplemental material). To examine how EutR functions in *C. rodentium*, we generated an *eutR* deletion strain. The Δ*eutR C. rodentium* strain was unable to grow using EA as a nitrogen source, and this defect could be complemented when *eutR* was expressed in *trans* (Fig. 1B). The Δ*eutR* growth defect was specific to EA utilization, as the wild-type (WT) and Δ*eutR* strains grew similarly in LB (Fig. S2). Genetic and biochemical studies with *Salmonella* and EHEC demonstrated that in response to EA and adenosylcobalamin, EutR promotes EA metabolism by binding to the *eutS* promoter to activate *eut*

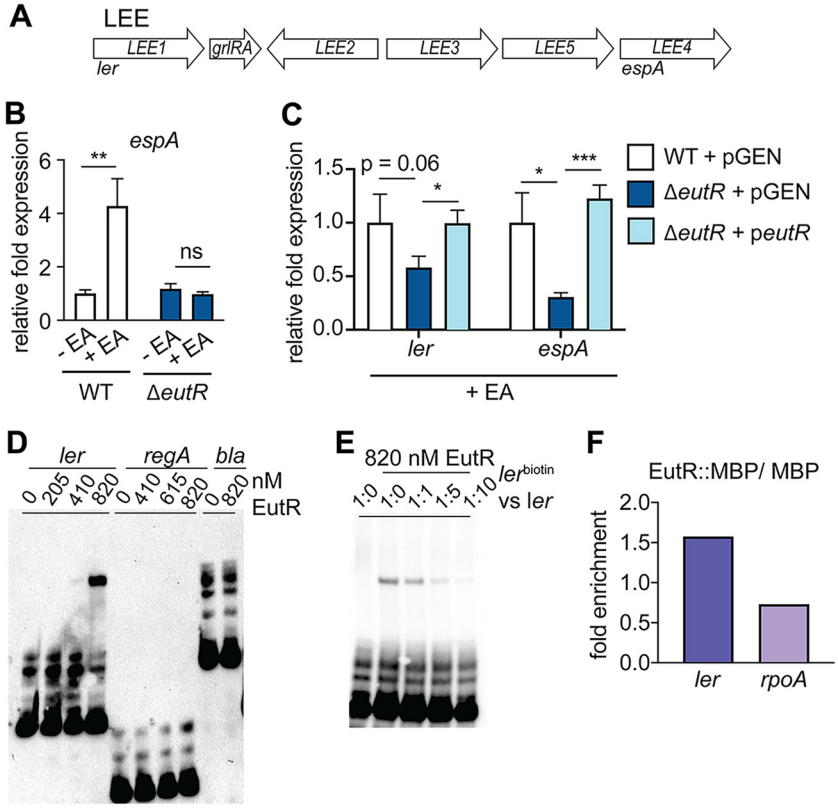

FIG 2 EA sensing and EutR-dependent LEE expression in *C. rodentium*. (A) Schematic of the LEE pathogenicity island. (B) RT-qPCR of *espA* expression in WT and Δ*eutR C. rodentium* in the absence or presence of EA ($n = 3$). (C) RT-qPCR of *ler* and *espA* expression in WT, Δ*eutR*, and complemented *C. rodentium* strains grown in the presence of EA ($n = 3$). (D) EMSA of *ler*, *regA*, and *bla* with EutR::MBP. (E) Competition EMSA using biotin-labeled and/or unlabeled *ler* probes. Ratios compare amount of labeled probe to amount of unlabeled probe. (F) qPCR showing enrichment of *ler* and *rpoA* from *in vivo* ChIP of EutR::MBP compared to MBP ($n = 2$). Error bars represent SD. *, $P < 0.05$; **, $P < 0.01$; ***, $P < 0.001$.

expression (17, 34, 36). Consistent with these data, in *C. rodentium*, EutR was required to sense EA and promote *eut* expression (Fig. 1C and D). Moreover, the *eutS* promoter of *C. rodentium* contains the EutR recognition sequence (17, 40). To further examine EutR regulation of the *eut* locus, we generated a plasmid expressing *C. rodentium* EutR fused to maltose-binding protein (MBP). After growth of the Δ*eutR* strain carrying the EutR::MBP or the empty MBP vector, EutR-DNA interactions were assessed using *in vivo* chromatin immunoprecipitation (ChIP). Using quantitative PCR (qPCR), we measured an enrichment of *eutS* in EutR::MBP samples compared to MBP alone (Fig. 1E). These data indicate that *C. rodentium* has maintained the ability to metabolize EA and that EutR is required for EA sensing and *eut* expression.

EutR promotes EA-dependent LEE expression in *C. rodentium*. EutR is important for EHEC to sense EA and activate expression of the LEE (16, 17). The LEE includes five major operons (41–43) (Fig. 2A). The T3SS filament protein is encoded by *espA*, which is carried in *LEE4*. Significantly, EA promoted *C. rodentium* virulence by enhancing expression of *espA* (Fig. 2B). Moreover, EutR was required for *C. rodentium* to sense EA and activate LEE expression, as the Δ*eutR* strain was unresponsive to the addition of EA to the culture medium (Fig. 2B). *ler* is the first gene within the *LEE1* operon (Fig. 2A) and encodes the master regulator of the LEE (43–46). Consistent with the case with EHEC, EutR was required for EA-dependent *ler* expression (Fig. 2C), and complementation of the Δ*eutR* strain restored LEE expression similar to WT levels (Fig. 2C).

To examine EutR interaction with the *ler* promoter, we purified EutR::MBP and performed electrophoretic mobility shift assays (EMSAs) using biotinylated *ler*, *regA*

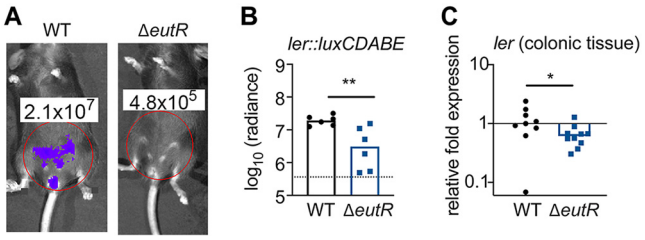

FIG 3 EutR enhances *C. rodentium* virulence gene expression *in vivo*. (A) Representative bioluminescent image of *ler* expression in mice infected with WT or Δ*eutR C. rodentium* at 10 dpi. (B) Quantification of bioluminescent data. (C) RT-qPCR of *ler* expression in WT and Δ*eutR C. rodentium* associated with colonic tissue. *, $P < 0.05$; **, $P < 0.01$.

(previously shown to influence LEE expression in *C. rodentium* [47]), and *bla* (negative control) probes. These assays indicated that EutR directly binds the *ler* promoter to activate expression of the LEE in a specific manner, as EutR did not bind either of the control probes *regA* and *bla* (Fig. 2D). Furthermore, MBP alone did not shift the *ler* promoter (Fig. S3). To confirm specificity of EutR interaction with the *ler* promoter, we performed a competition EMSA. Addition of an equal concentration of unlabeled *ler* probe competed with the ler^{biotin} probe for EutR binding, as visualized by decreased band intensity in shifted DNA compared to that for labeled probe alone (Fig. 2E). Furthermore, when added at increasing concentrations, the unlabeled probe completely outcompeted the labeled *ler* probe for EutR binding (Fig. 2E). To substantiate the *in vitro* data, we performed *in vivo* ChIP. In these experiments, we measured an enrichment of *ler* in EutR::MBP samples compared to MBP alone as well as compared to the negative control *rpoA* (Fig. 2F). These data demonstrate that EutR-dependent regulation of LEE expression is conserved in EHEC and *C. rodentium*.

EutR promotes *C. rodentium ler* expression during infection. The *in vitro* studies identified the LEE genes as EutR regulatory targets. We next tested the importance of EutR in controlling *ler* expression during intestinal infection. To do this, we constructed a transcriptional reporter in which the *ler* promoter was cloned upstream of the bacterial luciferase genes (Fig. S4A) and verified that this plasmid was retained during infection (Fig. S4B). At 10 days postinfection (dpi), *ler* expression was significantly decreased in the Δ*eutR* strain compared to that in the WT (Fig. 3A and B). To substantiate these data and control for potential differences in bacterial colonization, we infected mice with the WT or Δ*eutR* strain and harvested tissue at 10 dpi for transcriptional analyses of *ler* expression normalized to 16S rRNA expression. These data were consistent with data shown in Fig. 2, in which the *eutR* deletion resulted in a statistically significant (~2-fold) decrease in *ler* expression (Fig. 3C). Altogether, these data indicate that EutR is important for sensing the host environment and promoting LEE expression in the GI tract. Moreover, the magnitude differences in *ler* gene expression between WT and Δ*eutR* measured in whole colons versus normalized to *C. rodentium* CFU suggest that EutR affects pathogen burden in the intestine.

EutR is required for maximal *C. rodentium* fitness in the intestinal tract. The *C. rodentium* infection cycle in C57BL/6 mice is characterized by initial low levels of *C. rodentium*, followed by proliferation, and steady state, before clearance (Fig. 4A) (29). To examine how EutR affects *C. rodentium* colonization, we determined numbers of WT and Δ*eutR* strain CFU shed in stool throughout the infection cycle. Similar levels of Δ*eutR* and WT *C. rodentium* CFU were measured during the initial stages of infection. However, starting at 8 dpi and continuing until the end of the experiment, the Δ*eutR* strain was recovered at lower numbers than the WT (Fig. 4B). These findings reveal an important role for EutR in promoting colonization and persistence in the mammalian GI tract.

C. rodentium infection might affect EA levels in the intestine, which could be a contributing factor in the differences in colonization between the WT and Δ*eutR* strains

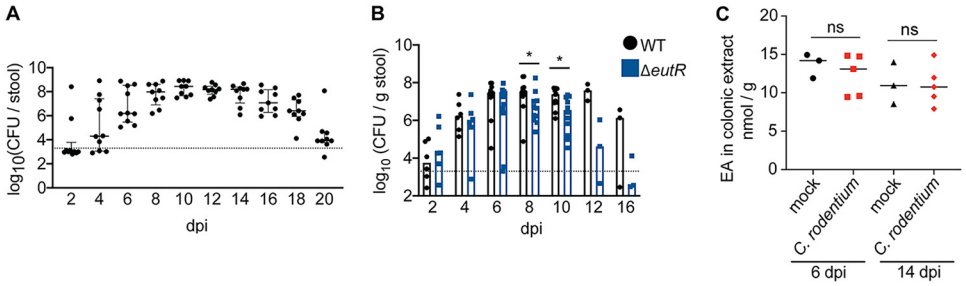

FIG 4 EutR is required for robust *C. rodentium* colonization independent of changes in EA availability. (A) CFU of WT *C. rodentium* shed in stool during infection. Data are presented as medians ± interquartile ranges. (B) CFU of WT and Δ*eutR C. rodentium* shed in stool. The dotted line represents the limit of detection. (C) EA levels in colons of mock-infected or WT *C. rodentium*-infected mice. *, $P < 0.05$.

measured during later stages of infection. To examine this possibility, we harvested whole colons from mock- or *C. rodentium*-infected mice at 6 and 14 dpi and measured EA levels in the tissue homogenates using liquid chromatography-mass spectrometry (LC-MS). At each time point, similar EA concentrations were measured from the colons of mice infected with 10^9 CFU of *C. rodentium* and mock-infected mice (Fig. 4C). These data suggest that *C. rodentium* infection does not alter EA concentrations in the intestine and that differences in WT and Δ*eutR* strain colonization are not due to changes in EA availability in the colon.

EutR is important for transmission efficiency. Passage through the GI tract results in a hypertransmissible state in which significantly fewer *C. rodentium* CFU are sufficient to cause infection than for bacteria cultivated *in vitro* (48). In C57BL/6 mice, ingestion of 10^7 to 10^8 CFU of freshly shed bacteria results in infection (48), compared to 10^9 CFU of *C. rodentium* grown in broth. At 10 dpi, the median CFU of the Δ*eutR* strain shed in stool was ~10-fold lower than the reported threshold that results in efficient transmission between animals. Therefore, we next investigated how EutR affects transmission. Following 24 h of cohousing with 6-dpi donor mice, equal numbers of WT and Δ*eutR C. rodentium* organisms were recovered in stool from recipient mice (Fig. 5A). In contrast, following cohousing with 10-dpi donor mice, the Δ*eutR* strain was recovered at significantly lower levels in stool of (formerly) naive mice (Fig. 5B and Fig. S5), indicating that EutR is important for pathogen persistence not only during primary infection but also within a host population.

Conclusions. Proper virulence gene expression in response to particular microenvironments is essential for pathogens to colonize a host (49). Our findings demonstrate that EutR is important for EA sensing and activation of LEE expression in *C. rodentium*, similar to its role in EHEC. Moreover, our findings reveal that EutR enhances virulence gene expression and colonization during infection of the GI tract.

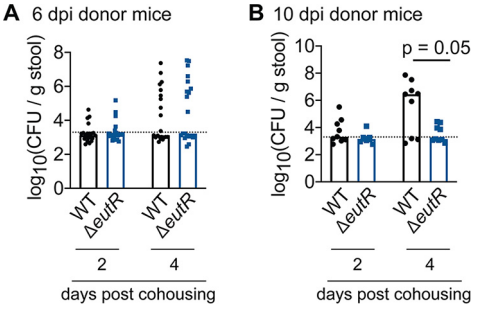

FIG 5 EutR promotes *C. rodentium* transmission. (A) CFU of WT and Δ*eutR C. rodentium* shed in stool of recipient mice following cohousing with 6-dpi donor mice. (B) CFU of WT and Δ*eutR C. rodentium* shed in stool of recipient mice following cohousing with 10-dpi donor mice.

EA is abundant in the intestinal tract due to the turnover of bacterial cells and exfoliation of enterocytes as well as through the host diet (2, 3). Although inflammation and infection have been suggested and/or shown to influence EA concentrations in the GI tract (13, 50), our data indicate that *C. rodentium* infection does not affect EA levels (Fig. 4C). Despite the consistent EA levels during infection, EutR affects *C. rodentium* virulence gene expression and colonization at later time points during infection (e.g., day 8 postinfection [Fig. 4B]), suggesting that spatiotemporal regulation of EutR expression and/or activity occurs in the GI tract. It is possible that EutR is part of a feed-forward regulatory circuit that integrates other environmental cues. For example, although *eutR* is constitutively expressed from the internal P2 promoter (36) (Fig. 1A), transcriptional regulation of this promoter may be more complex and include other transcription factors. Posttranscriptional regulation of *eutR* may also contribute to EutR expression. Alternatively, although EutR is required for EA sensing (6), EutR may not specifically respond to EA. In the complex *in vivo* environment, EutR may sense additional signals that affect spatiotemporal virulence gene regulation.

Notably, EutR not only is important for regulating expression of virulence traits in the attaching and effacing pathogens EHEC and *C. rodentium* but also plays a key role in regulating expression of *Salmonella* virulence traits required for survival and replication in macrophages (5, 6). These findings indicate a shared mechanism of host sensing and adaptation among distinct bacterial pathogens. Additionally, our findings suggest that EutR-dependent defects in pathogen colonization can be amplified during transmission and significantly impact the persistence of a pathogen within a host population. Together, these findings highlight the conserved role for EutR in promoting bacterial virulence and reveal new insights into the importance of EutR in host-to-host transmission, which is a poorly understood aspect of bacterial pathogenesis.

MATERIALS AND METHODS

Strains, plasmids, and recombinant DNA. *C. rodentium* DBS100 (51, 52) was used in this study. Primers are listed in Table S1. *C. rodentium* deletion strains were generated using λ-red mutagenesis (53). Briefly, PCR products were generated using pKD3 (Δ*lacZ*) or pKD4 (Δ*eutR*). The PCR products were transformed into *C. rodentium* expressing the λ-red genes from plasmid pKD46. The deletions were confirmed by sequencing. *C. rodentium* DBS100 lacks antibiotic resistance; therefore, we generated unresolved mutant strains for mouse infections. The Δ*lacZ* strain was used as the WT strain. Disruption of *lacZ* did not affect *C. rodentium* colonization of the GI tract (Fig. S6).

The *eutR* mutant was complemented using pGEN::*eutR*, which expressed *eutR* from the native promoter. This plasmid was constructed by amplifying *C. rodentium* genomic DNA (gDNA) using primers specific to the *eutR* gene, including 206 nucleotides upstream of the ATG start site. Amplified DNA was digested with NheI and SacI and inserted into pGEN-MCS (54) (Addgene MTA). As a control, the WT and Δ*eutR* strains were transformed with the empty pGEN-MCS vector.

Culture media. Bacteria were grown in Luria-Bertani medium (LB), Dulbecco's modified Eagle medium (DMEM; Invitrogen), or M9 minimal medium (55) that was supplemented with 10 mM EA hydrochloride (Sigma) as the sole nitrogen source. Cyanocobalamin (150 nM; Sigma) was added to the medium whenever EA was added. In general, bacteria were grown overnight (OVN) with shaking in LB at 37°C and then diluted 1:100 into fresh medium for experimental analysis.

EutR amino acid alignment. EutR sequences were obtained using the annotated EHEC EDL933 (56) and *C. rodentium* (57) genome sequences. The EMBOSS Needle program (58) was used to generate the alignment.

Transcriptional fusions. *C. rodentium* gDNA including the *ler* promoter, including 400 upstream and 43 nucleotides downstream of the ATG start site, was amplified by PCR. Resulting PCR products were cloned into the pGEN-*luxCDABE* vector (54) (Addgene MTA).

Purification of EutR under native conditions. The plasmid expressing EutR::MBP was constructed by amplifying the *eutR* gene from *C. rodentium* strain DBS100 using primers EutRMBP_F1 and EutRMBP_R1 and cloning the resulting PCR product into the NcoI/BamHI cloning sites of vector pMAL-c5X (New England BioLabs [NEB]). In order to purify MBP and EutR::MBP, *E. coli* strain BL-21(DE3) containing MBP or EutR::MBP was grown at 37°C in LB with glucose (0.2% [final concentration]) and ampicillin (100 μg/ml) to an optical density at 600 nm (OD_{600}) of 0.5. Then, isopropyl-β-D-thiogalactopyranoside (IPTG) was added to a final concentration of 0.3 mM, and protein expression was induced OVN at 18°C. Cells were harvested by centrifugation at 4,000 × *g* for 20 min, then resuspended in 25 ml of column buffer (20 mM Tris-HCl, 200 mM NaCl, 1 mM EDTA), and lysed by homogenization. The lysed cells were centrifuged, and the lysate was loaded onto a gravity column (Qiagen) with amylose resin. The column was washed with column buffer and then eluted with column buffer containing 10 mM maltose. Fractions containing purified proteins were confirmed by SDS-PAGE and Western blot analysis. Protein concentration was determined using a NanoDrop spectrophotometer.

ChIP-qPCR. Chromatin immunoprecipitation (ChIP) was performed using the *C. rodentium* Δ*eutR* strain transformed with pEutR::MBP or pMBP. Strains were grown in DMEM supplemented with EA, cyanocobalamin, and 2.5 μM IPTG until cells reached an OD_{600} of ~0.8. Cross-linking and ChIP were performed based on established methods (5, 59). After growth, formaldehyde was added (1% [final concentration]), and cells were incubated for 15 min at room temperature. Reactions were quenched with 0.5 M glycine, and then samples were pelleted, resuspended in phosphate-buffered saline (PBS), and washed. Cells were lysed with 2 mg/ml of lysozyme at 37°C for 30 min. Subsequently, samples were placed on ice and sonicated. Insoluble cell debris was removed by centrifugation, and supernatants were collected. RNase A was added to the samples, which were then incubated at 37°C for 1 h. One hundred units of Benzonase nuclease (EMD Millipore) was added to digest DNA into smaller fragments (60). Immunoprecipitation was performed using amylose beads (NEB) for 2 h at 4°C with gentle mixing. Beads were pelleted and washed. Then samples were incubated for 10 min at 65°C in elution buffer with occasional gentle mixing. Samples were centrifuged and supernatants were collected. To reverse the cross-link, samples were boiled for 10 min and DNA was purified using the Qiagen PCR purification kit. For ChIP-qPCR, an aliquot of each reaction was taken prior to immunoprecipitation, de-cross-linked by boiling for 10 min, and purified for use as the input control. The fold enrichment of each promoter represents the value of the immunoprecipitated DNA divided by the input unprecipitated DNA. These values were normalized to the values obtained for each promoter precipitated using MBP empty vector in order to account for nonspecific enrichment.

EMSAs. Electrophoretic mobility shift assays (EMSAs) were performed basically as described previously (5). We modified the protocol to use 5′-biotinylated primers to generate the labeled DNA probes. EMSAs were performed by adding increasing amounts of purified EutR protein to end-labeled probe (30 ng) in binding buffer (10 mM Tris-HCl [pH 8.0], 1 mM Na-EDTA, 80 mM NaCl, 10 mM β-mercaptoethanol, and 4% glycerol) (61), and reactions were incubated for 20 min at 37°C. For competition EMSAs, 25 ng of labeled probe was used with 0 ng, 25 ng, 125 ng, and 250 ng of unlabeled probe added. Immediately before the samples were loaded, Ficoll solution was added to the reaction mixtures. The samples were electrophoresed for approximately 4 to 5 h at 175 V on a 6% polyacrylamide gel, transferred to Zeta-Probe membranes, and visualized using the chemiluminescent nucleic acid detection module kit (Thermo Scientific).

Animal infections. All experiments were approved by the Institutional Animal Care and Use Committee at the University of Virginia School of Medicine. Female C57BL/6J (6- to 10-week-old) mice were inoculated by oral gavage of 1×10^9 CFU of *C. rodentium*. Mice were monitored daily for weight loss and other signs of distress. At the end of each experiment, mice were euthanized by CO_2 asphyxiation followed by cervical dislocation.

Enumeration of CFU from stool. For enumeration of CFU from stool, fresh fecal pellets were collected at the desired time points, weighed, and homogenized in 1 ml of PBS. Serial dilutions were plated on LB plates containing appropriate antibiotic selectivity to evaluate CFU. Enumerated CFU per gram of stool were log transformed prior to statistical analysis, as previously described (62).

RNA extraction and RT-qPCR. Bacterial cells grown *in vitro* were resuspended in TRIzol (Life Technologies). Colonic tissue was harvested, washed with PBS to remove luminal contents, and then homogenized in TRIzol. For all samples, RNA was extracted using a PureLink RNA minikit (Invitrogen). Reverse transcription-qPCR (RT-qPCR; for *in vitro* and colonic samples) was performed as previously described (63) in a one-step reaction using an ABI 7500-FAST sequence detection system and software (Applied Biosystems). For each 10-μl reaction mixture, 5 μl of 2× SYBR master mix (Ambion), 0.05 μl of Multi-Scribe reverse transcriptase (Invitrogen), and 0.05 μl of RNase inhibitor (Invitrogen) were added. For stool samples, cDNA was synthesized using SuperScript II reverse transcriptase (Invitrogen) with random primers prior to qPCR to overcome low RNA yields. Reactions are identical to those described for RT-qPCR omitting reverse transcriptase and adjustment for a final 10-μl volume. Primers were designed using Primer BLAST (NCBI) to ensure no cross-reactivity to other genes in the *C. rodentium* chromosome. Amplicon length was approximately 100 bp. Amplification efficiency of each primer pair was verified using standard curves of known DNA concentrations. Melting-curve analysis was used to ensure template specificity by heating products to 95°C for 15 s, followed by cooling to 60°C and heating to 95°C while monitoring fluorescence. After the amplification efficiency and template specificity were determined for each primer pair, relative quantification analysis was used to analyze the samples using the following conditions for cDNA generation and amplification: 1 cycle at 48°C for 30 min, 1 cycle at 95°C for 10 min, and 40 cycles at 95°C for 15 s and 60°C for 1 min. Two technical replicates of each biological replicate were included for each gene target. Data were normalized to the reference controls *rpoA* (*in vitro* samples) or 16S rRNA specific to *C. rodentium* (tissue samples) and analyzed using the comparative critical threshold (C_T) method (64). The expression levels of the target genes were compared using the relative quantification method (64).

EA measurements. EA levels were measured as previously described (13), with minor modifications. Colons were harvested, weighed, and homogenized in 1.5 ml of ultrapure water. Homogenized tissue was incubated with 150 μl of 40% sulfosalicylic acid (Sigma) for 15 min and then centrifuged at 11,000 × *g* for 15 min at room temperature. Then 1 ml of the supernatant was mixed with 300 μl of 0.5 M $NaHCO_3$ (Sigma), 2 ml of 20-mg/ml dansyl chloride solution (Sigma) in acetone, and 200 μl of 1 M NaOH (Fisher). Following incubation in the dark for 20 min at room temperature, 200 μl of 25% NH_4OH (Sigma) was added. The volume was adjusted to 5 ml with acetonitrite (Sigma), and 1 ml was centrifuged at 11,000 × *g* for 1 min. The supernatant was taken for analysis. The LC-MS system consists of a ThermoElectron Orbitrap ID-X mass spectrometer with a Heated Electrospray Ionization source interfaced to a Thermo Accucore Vanquish C_{18} 1.5-μm, 2.1- by 100-mm column. Two microliters of the extract was

injected and the compounds were eluted from the column by a methanol-0.1% formic acid gradient at a flow rate of 250 μl/min (total time, 15 min). The nanospray ion source was operated at 3.2 kV. The sample was analyzed by MS and tandem MS (MS/MS). The dansyl-EA was detected as a peak at ~4.36 min and a mass of 295.111+. A 1 M *in vitro* sample of EA hydrochloride (Sigma) taken through the dansylation process was used to generate a standard curve.

***In vivo* imaging system (IVIS) analysis.** For *in vivo* bioluminescence on living mice, an IVIS Spectrum (Caliper Lifesciences, Alameda, CA) was used. Luminescence (radiance) was quantified using the software program Living Image (Xenogen). Radiance is reported as photons per second.

Transmission studies. Donor mice were infected with WT or Δ*eutR C. rodentium* for 6 or 10 days. At these time points, each donor mouse was placed in a fresh cage with 3 naive mice for 24 h. For data shown in Fig. 5, at 24 h after cohousing, all mice were separated and placed in fresh, individual cages. For data shown in Fig. S5, respective recipient mice were cohoused after exposure to donor mice. At 2 or 4 days after cohousing with donor mice, stool was collected from each recipient mouse, homogenized in PBS, and plated on appropriate selective media to determine CFU of transmitted *C. rodentium*.

Statistical analyses. Statistical analyses were performed using GraphPad Prism software version 8.0 (GraphPad Software Inc.). Group comparisons were performed using Student's *t* test for *in vitro* analyses and the Wilcoxon signed-rank test for all *in vivo* analyses.

SUPPLEMENTAL MATERIAL

Supplemental material is available online only.

SUPPLEMENTAL FILE 1, PDF file, 0.1 MB.

SUPPLEMENTAL FILE 2, PDF file, 0.1 MB.

SUPPLEMENTAL FILE 3, PDF file, 0.5 MB.

SUPPLEMENTAL FILE 4, PDF file, 0.2 MB.

SUPPLEMENTAL FILE 5, PDF file, 0.1 MB.

SUPPLEMENTAL FILE 6, PDF file, 0.1 MB.

SUPPLEMENTAL FILE 7, PDF file, 0.02 MB.

ACKNOWLEDGMENTS

We thank members of the Kendall lab for thoughtful discussions on this work and Hervé Agaisse for feedback on the manuscript. We thank Sarah Ewald for advice on the IVIS experiments and James Nataro for the *Citrobacter rodentium* DBS100 strain. We thank the Biomolecular Analysis Facility at the University of Virginia for LC-MS and analysis services.

This work was supported by National Institutes of Health NIAID grants AI118732, AI130439, and AI146888 to M.M.K. C.A.R. received support from NIH training grant 5T32AI007046 and a UVA Wagner Fellowship. A.B.S. received support from NIH training grant 5T32AI055432.

The funders had no role in study design, data collection and interpretation, or the decision to submit the work for publication.

REFERENCES

1. Luzader DH, Kendall MM. 2016. Commensal 'trail of bread crumbs' provide pathogens with a map to the intestinal landscape. Curr Opin Microbiol 29:68–73. https://doi.org/10.1016/j.mib.2015.11.005.
2. Cotton PB. 1972. Non-dietary lipid in the intestinal lumen. Gut 13:675–681. https://doi.org/10.1136/gut.13.9.675.
3. Garsin DA. 2010. Ethanolamine utilization in bacterial pathogens: roles and regulation. Nat Rev Microbiol 8:290–295. https://doi.org/10.1038/nrmicro2334.
4. Snoeck V, Goddeeris B, Cox E. 2005. The role of enterocytes in the intestinal barrier function and antigen uptake. Microbes Infect 7:997–1004. https://doi.org/10.1016/j.micinf.2005.04.003.
5. Anderson CJ, Clark DE, Adli M, Kendall MM. 2015. Ethanolamine signaling promotes *Salmonella* niche recognition and adaptation during infection. PLoS Pathog 11:e1005278. https://doi.org/10.1371/journal.ppat.1005278.
6. Anderson CJ, Satkovich J, Köseoğlu V, Agaisse H, Kendall MM. 2018. The ethanolamine permease EutH promotes vacuole adaptation of *Salmonella enterica* and *Listeria monocytogenes* during macrophage infection. Infect Immun 86:e00172-18. https://doi.org/10.1128/IAI.00172-18.
7. Bertin Y, Girardeau JP, Chaucheyras-Durand F, Lyan B, Pujos-Guillot E, Harel J, Martin C. 2011. Enterohaemorrhagic *Escherichia coli* gains a competitive advantage by using ethanolamine as a nitrogen source in the bovine intestinal content. Environ Microbiol 13:365–377. https://doi.org/10.1111/j.1462-2920.2010.02334.x.
8. Maadani A, Fox KA, Mylonakis E, Garsin DA. 2007. *Enterococcus faecalis* mutations affecting virulence in *Caenorhabditis elegans* model host. Infect Immun 75:2634–2637. https://doi.org/10.1128/IAI.01372-06.
9. Mellin JR, Koutero M, Dar D, Nahori MA, Sorek R, Cossart P. 2014. Riboswitches. Sequestration of a two-component response regulator by a riboswitch-regulated noncoding RNA. Science 345:940–943. https://doi.org/10.1126/science.1255083.
10. Nawrocki KL, Wetzel D, Jones JB, Woods EC, McBride SM. 2018. Ethanolamine is a valuable nutrient source that impacts *Clostridium difficile* pathogenesis. Environ Microbiol 20:1419–1435. https://doi.org/10.1111/1462-2920.14048.
11. Rowley CA, Anderson CJ, Kendall MM. 2018. Ethanolamine influences human commensal *Escherichia coli* growth, gene expression, and competition with enterohemorrhagic *E. coli* O157:H. mBio 9:e01429-18. https://doi.org/10.1128/mBio.01429-18.
12. Sintsova A, Smith S, Subashchandrabose S, Mobley HL. 2018. Role of ethanolamine utilization genes in host colonization during urinary tract infection. Infect Immun 86:e00542-17. https://doi.org/10.1128/IAI.00542-17.
13. Thiennimitr P, Winter SE, Winter MG, Xavier MN, Tolstikov V, Huseby DL,

Sterzenbach T, Tsolis RM, Roth JR, Bäumler AJ. 2011. Intestinal inflammation allows *Salmonella* to use ethanolamine to compete with the microbiota. Proc Natl Acad Sci U S A 108:17480–17485. https://doi.org/10.1073/pnas.1107857108.
14. Yagi H, Nakayama-Imaohji H, Nariya H, Tada A, Yamasaki H, Ugai H, Elahi M, Ono T, Kuwahara T. 2018. Ethanolamine utilization supports *Clostridium perfringens* growth in infected tissues. Microb Pathog 119:200–207. https://doi.org/10.1016/j.micpath.2018.04.017.
15. Gonyar LA, Kendall MM. 2014. Ethanolamine and choline promote expression of putative and characterized fimbriae in enterohemorrhagic *Escherichia coli* O157:H7. Infect Immun 82:193–201. https://doi.org/10.1128/IAI.00980-13.
16. Kendall MM, Gruber CC, Parker CT, Sperandio V. 2012. Ethanolamine controls expression of genes encoding components involved in interkingdom signaling and virulence in enterohemorrhagic *Escherichia coli* O157:H7. mBio 3:e00050-12. https://doi.org/10.1128/mBio.00050-12.
17. Luzader DH, Clark DE, Gonyar LA, Kendall MM. 2013. EutR is a direct regulator of genes that contribute to metabolism and virulence in enterohemorrhagic *Escherichia coli* O157:H7. J Bacteriol 195:4947–4953. https://doi.org/10.1128/JB.00937-13.
18. Karmali MA. 2004. Infection by Shiga toxin-producing *Escherichia coli*. Mol Biotechnol 26:117–122. https://doi.org/10.1385/MB:26:2:117.
19. Karmali MA, Petric M, Lim C, Fleming PC, Steele BT. 1983. *Escherichia coli* cytotoxin, haemolytic-uraemic syndrome, and haemorrhagic colitis. Lancet ii:1299–1300. https://doi.org/10.1016/s0140-6736(83)91167-4.
20. Elliott SJ, Krejany EO, Mellies JL, Robins-Browne RM, Sasakawa C, Kaper JB. 2001. EspG, a novel type III system-secreted protein from enteropathogenic *Escherichia coli* with similarities to VirA of *Shigella flexneri*. Infect Immun 69:4027–4033. https://doi.org/10.1128/IAI.69.6.4027-4033.2001.
21. Jarvis KG, Giron JA, Jerse AE, McDaniel TK, Donnenberg MS, Kaper JB. 1995. Enteropathogenic *Escherichia coli* contains a putative type III secretion system necessary for the export of proteins involved in attaching and effacing lesion formation. Proc Natl Acad Sci U S A 92:7996–8000. https://doi.org/10.1073/pnas.92.17.7996.
22. Jerse AE, Yu J, Tall BD, Kaper JB. 1990. A genetic locus of enteropathogenic *Escherichia coli* necessary for the production of attaching and effacing lesions on tissue culture cells. Proc Natl Acad Sci U S A 87:7839–7843. https://doi.org/10.1073/pnas.87.20.7839.
23. Kanack KJ, Crawford JA, Tatsuno I, Karmali MA, Kaper JB. 2005. SepZ/EspZ is secreted and translocated into HeLa cells by the enteropathogenic *Escherichia coli* type III secretion system. Infect Immun 73:4327–4337. https://doi.org/10.1128/IAI.73.7.4327-4337.2005.
24. Kenny B, DeVinney R, Stein M, Reinscheid DJ, Frey EA, Finlay BB. 1997. Enteropathogenic *E. coli* (EPEC) transfers its receptor for intimate adherence into mammalian cells. Cell 91:511–520. https://doi.org/10.1016/S0092-8674(00)80437-7.
25. Kenny B, Jepson M. 2000. Targeting of an enteropathogenic *Escherichia coli* (EPEC) effector protein to host mitochondria. Cell Microbiol 2:579–590. https://doi.org/10.1046/j.1462-5822.2000.00082.x.
26. Kenny B, Lai L-C, Finlay BB, Donnenberg MS. 1996. EspA, a protein secreted by enteropathogenic *Escherichia coli*, is required to induce signals in epithelial cells. Mol Microbiol 20:313–323. https://doi.org/10.1111/j.1365-2958.1996.tb02619.x.
27. McNamara BP, Donnenberg MS. 1998. A novel proline-rich protein, EspF, is secreted from enteropathogenic *Escherichia coli* via the type III export pathway. FEMS Microbiol Lett 166:71–78. https://doi.org/10.1111/j.1574-6968.1998.tb13185.x.
28. Kaper JB, Nataro JP, Mobley HL. 2004. Pathogenic *Escherichia coli*. Nat Rev Microbiol 2:123–140. https://doi.org/10.1038/nrmicro818.
29. Mullineaux-Sanders C, Sanchez-Garrido J, Hopkins EGD, Shenoy AR, Barry R, Frankel G. 2019. *Citrobacter rodentium*-host-microbiota interactions: immunity, bioenergetics and metabolism. Nat Rev Microbiol 17:701–715. https://doi.org/10.1038/s41579-019-0252-z.
30. Collins JW, Keeney KM, Crepin VF, Rathinam VAK, Fitzgerald KA, Finlay BB, Frankel G. 2014. *Citrobacter rodentium*: infection, inflammation, and the microbiota. Nat Rev Microbiol 12:612–623. https://doi.org/10.1038/nrmicro3315.
31. Mundy R, MacDonald TT, Dougan G, Frankel G, Wiles S. 2005. *Citrobacter rodentium* of mice and man. Cell Microbiol 7:1697–1706. https://doi.org/10.1111/j.1462-5822.2005.00625.x.
32. Deng W, Li Y, Vallance BA, Finlay BB. 2001. Locus of enterocyte effacement from *Citrobacter rodentium*: sequence analysis and evidence for horizontal transfer among attaching and effacing pathogens. Infect Immun 69:6323–6335. https://doi.org/10.1128/IAI.69.10.6323-6335.2001.
33. Kofoid E, Rappleye C, Stojiljkovic I, Roth J. 1999. The 17-gene ethanolamine (*eut*) operon of *Salmonella typhimurium* encodes five homologues of carboxysome shell proteins. J Bacteriol 181:5317–5239. https://doi.org/10.1128/JB.181.17.5317-5329.1999.
34. Roof DM, Roth JR. 1988. Ethanolamine utilization in *Salmonella typhimurium*. J Bacteriol 170:3855–3863. https://doi.org/10.1128/jb.170.9.3855-3863.1988.
35. Roof DM, Roth JR. 1989. Functions required for vitamin B12-dependent ethanolamine utilization in *Salmonella typhimurium*. J Bacteriol 171:3316–3323. https://doi.org/10.1128/jb.171.6.3316-3323.1989.
36. Roof DM, Roth JR. 1992. Autogenous regulation of ethanolamine utilization by a transcriptional activator of the *eut* operon in *Salmonella typhimurium*. J Bacteriol 174:6634–6643. https://doi.org/10.1128/jb.174.20.6634-6643.1992.
37. Sheppard DE, Penrod JT, Bobik T, Kofoid E, Roth JR. 2004. Evidence that a B12-adenosyl transferase is encoded within the ethanolamine operon of *Salmonella enterica*. J Bacteriol 186:7635–7644. https://doi.org/10.1128/JB.186.22.7635-7644.2004.
38. Stojiljkovic I, Bäumler AJ, Heffron F. 1995. Ethanolamine utilization in *Salmonella typhimurium:* nucleotide sequence, protein expression, and mutational analysis of the *cchA cchB eutE eutJ eutG eutH* gene cluster. J Bacteriol 177:1357–1366. https://doi.org/10.1128/jb.177.5.1357-1366.1995.
39. Segura A, Auffret P, Klopp C, Bertin Y, Forano E. 2017. Draft genome sequence and characterization of commensal *Escherichia coli* strain BG1 isolated from bovine gastro-intestinal tract. Stand Genomic Sci 12:61. https://doi.org/10.1186/s40793-017-0272-0.
40. Tsoy O, Ravcheev D, Mushegian A. 2009. Comparative genomics of ethanolamine utilization. J Bacteriol 191:7157–7164. https://doi.org/10.1128/JB.00838-09.
41. Elliott SJ, Hutcheson SW, Dubois MS, Mellies JL, Wainwright L, Batchelor M, Frankel G, Knutton S, Kaper JB. 1999. Identification of CesT, a chaperone for the type III secretion of Tir in enteropathogenic *Escherichia coli*. Mol Microbiol 33:1176–1189. https://doi.org/10.1046/j.1365-2958.1999.01559.x.
42. Elliott SJ, Wainwright L, McDaniel TK, Jarvis KG, Deng YK, Lai L-C, McNamara BP, Donnenberg MS, Kaper JB. 1998. The complete sequence of the locus of enterocyte effacement (LEE) from enteropathogenic *Escherichia coli* E2348/69. Mol Microbiol 28:1–4. https://doi.org/10.1046/j.1365-2958.1998.00783.x.
43. Mellies JL, Elliott SJ, Sperandio V, Donnenberg MS, Kaper JB. 1999. The Per regulon of enteropathogenic *Escherichia coli*: identification of a regulatory cascade and a novel transcriptional activator, the locus of enterocyte effacement (LEE)-encoded regulator (Ler). Mol Microbiol 33:296–306. https://doi.org/10.1046/j.1365-2958.1999.01473.x.
44. Haack KR, Robinson CL, Miller KJ, Fowlkes JW, Mellies JL. 2003. Interaction of Ler at the LEE5 (tir) operon of enteropathogenic *Escherichia coli*. Infect Immun 71:384–392. https://doi.org/10.1128/iai.71.1.384-392.2003.
45. Sánchez-SanMartín C, Bustamante VH, Calva E, Puente JL. 2001. Transcriptional regulation of the *orf19* gene and the *tir-cesT-eae* operon of enteropathogenic *Escherichia coli*. J Bacteriol 183:2823–2833. https://doi.org/10.1128/JB.183.9.2823-2833.2001.
46. Sperandio V, Mellies JL, Delahay RM, Frankel G, Crawford JA, Nguyen W, Kaper JB. 2000. Activation of enteropathogenic *Escherichia coli* (EPEC) LEE2 and LEE3 operons by Ler. Mol Microbiol 38:781–793. https://doi.org/10.1046/j.1365-2958.2000.02168.x.
47. Tan A, Petty NK, Hocking D, Bennett-Wood V, Wakefield M, Praszkier J, Tauschek M, Yang J, Robins-Browne RM. 2015. Evolutionary adaptation of an AraC-like regulatory protein in *Citrobacter rodentium* and *Escherichia* species. Infect Immun 83:1384–1395. https://doi.org/10.1128/IAI.02697-14.
48. Wiles S, Dougan G, Frankel G. 2005. Emergence of a 'hyperinfectious' bacterial state after passage of *Citrobacter rodentium* through the host gastrointestinal tract. Cell Microbiol 7:1163–1172. https://doi.org/10.1111/j.1462-5822.2005.00544.x.
49. Barnett-Foster DE. 2013. Modulation of the enterohemorrhagic *E. coli* virulence program through the human gastrointestinal tract. Virulence 4:315–323. https://doi.org/10.4161/viru.24318.
50. Ormsby MJ, Logan M, Johnson SA, McIntosh A, Fallata G, Papadopoulou R, Papachristou E, Hold GL, Hansen R, Ijaz UZ, Russell RK, Gerasimidis K, Wall DM. 2019. Inflammation associated ethanolamine facilitates infection by Crohn's disease-linked adherent-invasive *Escherichia coli*. EBioMedicine 43:325–332. https://doi.org/10.1016/j.ebiom.2019.03.071.

51. Schauer DB, Falkow S. 1993. Attaching and effacing locus of a *Citrobacter freundii* biotype that causes transmissible murine colonic hyperplasia. Infect Immun 61:2486–2492. https://doi.org/10.1128/IAI.61.6.2486-2492.1993.
52. Barthold SW, Coleman GL, Bhatt PN, Osbaldiston GW, Jonas AM. 1976. The etiology of transmissible murine colonic hyperplasia. Lab Anim Sci 26:889–894.
53. Datsenko KA, Wanner BL. 2000. One-step inactivation of chromosomal genes in Escherichia coli K-12 using PCR products. Proc Natl Acad Sci U S A 97:6640–6645. https://doi.org/10.1073/pnas.120163297.
54. Lane MC, Alteri CJ, Smith SN, Mobley HL. 2007. Expression of flagella is coincident with uropathogenic Escherichia coli ascension to the upper urinary tract. Proc Natl Acad Sci U S A 104:16669–16674. https://doi.org/10.1073/pnas.0607898104.
55. Sambrook J, Fritsch EF, Maniatis T. 1989. Molecular cloning: a laboratory manual, 2nd ed. Cold Spring Harbor Laboratory Press, Cold Spring Harbor, NY.
56. Perna NT, Plunkett G, Burland V, Mau B, Glasner JD, Rose DJ, Mayhew GF, Evans PS, Gregor J, Kirkpatrick HA, Pósfai G, Hackett J, Klink S, Boutin A, Shao Y, Miller L, Grotbeck EJ, Davis NW, Lim A, Dimalanta ET, Potamousis KD, Apodaca J, Anantharaman TS, Lin J, Yen G, Schwartz DC, Welch RA, Blattner FR. 2001. Genome sequence of enterohaemorrhagic *Escherichia coli* O157:H7. Nature 409:529–533. https://doi.org/10.1038/35054089.
57. Petty NK, Bulgin R, Crepin VF, Cerdeño-Tárraga AM, Schroeder GN, Quail MA, Lennard N, Corton C, Barron A, Clark L, Toribio AL, Parkhill J, Dougan G, Frankel G, Thomson NR. 2010. The *Citrobacter rodentium* genome sequence reveals convergent evolution with human pathogenic *Escherichia coli*. J Bacteriol 192:525–538. https://doi.org/10.1128/JB.01144-09.
58. Madeira F, Park YM, Lee J, Buso N, Gur T, Madhusoodanan N, Basutkar P, Tivey ARN, Potter SC, Finn RD, Lopez R. 2019. The EMBL-EBI search and sequence analysis tools APIs in 2019. Nucleic Acids Res 47:W636–W641. https://doi.org/10.1093/nar/gkz268.
59. Rhodius VA, Wade JT. 2009. Technical considerations in using DNA microarrays to define regulons. Methods 47:63–72. https://doi.org/10.1016/j.ymeth.2008.10.017.
60. Pchelintsev NA, Adams PD, Nelson DM. 2016. Critical parameters for efficient sonication and improved chromatin immunoprecipitation of high molecular weight proteins. PLoS One 11:e0148023. https://doi.org/10.1371/journal.pone.0148023.
61. Santiago AE, Yan MB, Hazen TH, Sauder AB, Meza-Segura M, Rasko DA, Kendall MM, Ruiz-Perez F, Nataro JP. 2017. The AraC negative regulator family modulates the activity of histone-like proteins in pathogenic bacteria. PLoS Pathog 13:e1006545. https://doi.org/10.1371/journal.ppat.1006545.
62. Lopez CA, Miller BM, Rivera-Chávez F, Velazquez E, Byndloss MX, Chávez-Arroyo A, Lokken KL, Tsolis RM, Winter SE, Bäumler AJ. 2016. Virulence factors enhance *Citrobacter rodentium* expansion through aerobic respiration. Science 353:1249–1253. https://doi.org/10.1126/science.aag3042.
63. Melson EM, Kendall MM. 2019. The sRNA DicF integrates oxygen sensing to enhance enterohemorrhagic *Escherichia coli* virulence via distinctive RNA control mechanisms. Proc Natl Acad Sci U S A 116:14210–14215. https://doi.org/10.1073/pnas.1902725116.
64. Livak KJ. 1997. ABI Prism 7700 sequence detection system. User bulletin no 2, PE Applied Biosystems 4303859B:777802–778002.